Progress In Electromagnetics Research, PIER 98, 359–373, 2009

NUMERICAL CALCULATIONS ON INCLUSION REMOVAL FROM LIQUID METALS UNDER STRONG MAGNETIC FIELDS

Z. Sun, M. Guo, J. Vleugels, O. Van Der Biest, and B. Blanpain

Department of Metallurgy and Materials Engineering
Katholieke Universiteit Leuven
Kasteelpark Arenberg 44, Heverlee (Leuven) BE-3001, Belgium

Abstract—A numerical method is developed to calculate/simulate the separation of non-metallic inclusions from an aluminum melt by using a strong magnetic field (e.g., 10 Tesla) with high gradient generated via a superconducting magnet. The cases with and without imposed DC current on liquid aluminum in a cylindrical channel are discussed and compared. The migrating velocities of the non-metallic inclusions in an aluminum melt are calculated through force analysis and Navier-Stokes equations. In addition, the trajectories and removal efficiencies of the inclusions are evaluated. It is found that particle trajectories are influenced by the imposed flow rate and inclusion particle size. In addition, the removal efficiency is improved significantly, especially for small inclusions, e.g., $< 10\,\mu$m, by an imposed DC current on liquid aluminum in the high gradient area of a magnetic field.

1. INTRODUCTION

Increasing demand of high quality aluminum metal and its alloys promotes the development of non-metallic inclusions separation technologies from liquid aluminum [1, 2]. The presence of inclusions can strongly influence the mechanical properties and corrosion resistance of the aluminum parts in performance [3]. A range of methods have been proposed for the removal of inclusions during the aluminum secondary refining process. Traditionally, the methods include flotation or sedimentation; ceramic filtration; bubbling capture; and stirring or centrifugal separation [1–4]. Many studies with respect to these technologies have been reported and some have been applied in

Corresponding author: Z. Sun (zhisun@126.com).

industry. However, small sized inclusions are still difficult to be removed.

Recently, electromagnetic fields have been applied to separate inclusions from liquid metal during its secondary refining process [1, 5–10]. Treatment by using a strong magnetic field with high gradient is considered to be a power efficient method [11]. Due to the rapid development of superconducting technologies, strong magnetic fields of, e.g., 10 T, can nowadays be easily obtained. Under strong magnetic fields, the magnetisation forces become considerable even for small gas bubbles on which the forces are, however, negligible under lower magnetic fields. Meanwhile, the magnitude of the Lorentz force density with an imposed current can also be considerably increased by an increase of the magnetic field intensity, facilitating the removal of small particles. A possible method, combining the Lorentz and magnetisation forces, has been proposed to remove small inclusions of around 10 µm [11]. However, there is still lack of detailed descriptions of the effect of a strong magnetic field and reports on the operational parameters for small inclusion removal are limited.

In the present paper, a numerical method is conducted to assess the inclusion removal from a liquid metal (we introduced aluminum melt as an example) in a strong magnetic field with a high gradient and with an imposed DC current in a cylindrical channel. The specific case of liquid aluminum is considered. Combining the electromagnetic theories and fluid dynamics, the particle migration velocities and trajectories are evaluated and compared for the cases with and without the imposed current. In addition, removal efficiencies are estimated. A process to remove small inclusions from liquid metal by applying strong magnetic fields and a DC current is proposed.

2. THEORY AND NUMERICAL MODEL

A schematic diagram of the inclusion removal by using a strong magnetic field with a high gradient is shown in Fig. 1. The superconducting magnet bore is 150 mm in diameter with a high gradient area, in which, the cylindrical channel (the dimensions are shown in Fig. 1) is located. The aluminum melt containing non-metallic inclusions flows through the channel with a constant inlet velocity v_M. A DC current in the axial direction of the channel with a constant density, $\vec{J}$ (A/m^2), is imposed. The physical properties of the liquid aluminum and some non-metallic inclusion particles are listed in Table 1 [12]. Both cases with and without the imposed current were considered in the calculations.

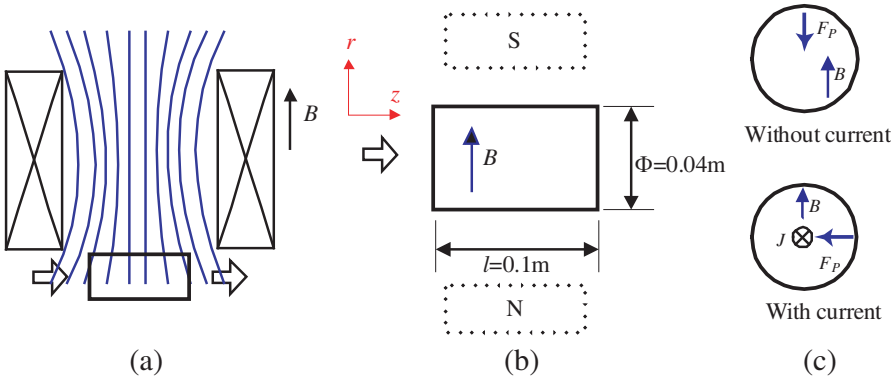

Figure 1. Schematic diagram of the principle of inclusion removal from flowing melt in a cylindrical channel under a strong magnetic field with high gradient (the channel is placed in the high gradient area with the channel axis perpendicular to the magnetic field direction). (a) The whole image; (b) the axial image of the channel; and (c) the cross-section of the channel (F_P is the force on the inclusion particle).

Table 1. Physical properties of liquid aluminum at 933 K and some non-metallic inclusion particles.

	χ, 10^{-5}	Density, kg/m^3	Viscosity, 10^{-3} Pa· S	Electrical conductivity, $10^6(\Omega \cdot \mathrm{m})^{-1}$
Al	1.323	2370	1.25	4.1322
Al_2O_3	−1.81	3970		
SiC	−1.29	3220		
SiO_2	−1.65	2660		

2.1. Inclusion Removal from Liquid Aluminum under a Strong Magnetic Field with a High Gradient

Under a vertical strong magnetic field with high gradient, a non-metallic inclusion experiences gravity, buoyancy, Faraday, and Stokes viscosity drag forces. The force analysis is schematically shown in Fig. 2 and the detailed derivation is provided elsewhere [13].

According to Fig. 2, the resultant force can be expressed by

$$F_p - F_{\eta,B} = \Delta F_m + \Delta G - F_{\eta,B} \tag{1}$$

where F_p is the driving force and ΔF_m is the resultant Faraday force on the non-metallic inclusion, ΔG is the difference between the gravity and buoyancy forces and $F_{\eta,B}$ is the Stokes viscosity drag force for

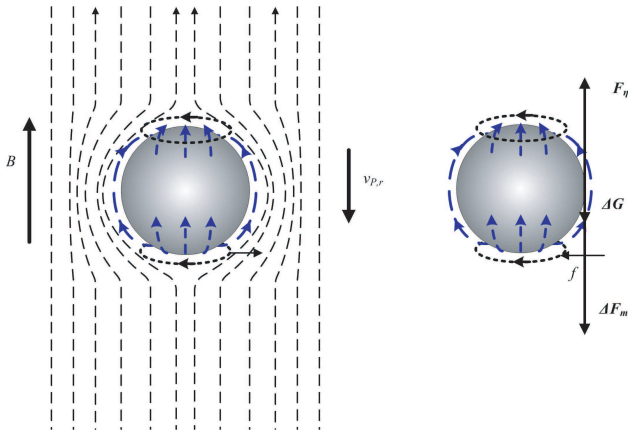

Figure 2. Schematic plot of the force analysis on a non-metallic inclusion.

laminar flow.

$$\Delta G = V(\rho_p - \rho_M)g \tag{2}$$

where ρ_M and ρ_p are the densities of the liquid melt and of the non-metallic inclusion, respectively, g is the gravitational constant, V is the volume of the particle.

$$\Delta F_m = V(\chi_M - \chi_p)\frac{1}{\mu_0}B\nabla B \tag{3}$$

where μ_0 ($= 4\pi \times 10^{-7}\,\mathrm{Hm}^{-1}$) is the magnetic permeability of vacuum, χ_M and χ_p are respectively the volumetric mass magnetic susceptibility of the liquid melt and the diamagnetic/paramagnetic particle; B and ∇B denote the magnetic field density and magnetic field gradient respectively.

For a spherical particle with Reynolds number less than 1, the Stokes drag force is

$$F_{\eta,B} = 3\pi\eta_{M,B}v_{P,r}d_p \tag{4}$$

where $\eta_{M,B}$ is the viscosity of the melt in a strong magnetic field, $v_{P,r}$ is the inclusion velocity in radial r direction and d_p is the inclusion diameter.

Under a strong magnetic field, a local flow of liquid melt induced by the migration of the inclusion particle cuts the magnetic field lines and induces current as well as a local Lorentz force f (see Fig. 2) on the flowing liquid melt. The local Lorentz force acts as a pressure on the bottom surface of the settling particle, resulting in a contribution to the viscosity drag force. Therefore, the melt viscosity is considered

to be influenced by the magnetic field. The viscosity of the melt in the strong magnetic field can be derived from the Hartmann number (Ha).

$$\begin{aligned}\eta_{M,B} &\cong \frac{1}{3}\eta_M Ha \quad (Ha \gg 1)\\ &\cong \eta_M\left(1+\frac{3}{8}Ha\right) \quad (Ha \ll 1)\\ &\cong \eta_M\left(\frac{1+\frac{11}{8}Ha+\frac{1}{3}Ha^2}{1+Ha}\right) \quad (Ha \approx 1)\end{aligned} \tag{5}$$

where $Ha = B\frac{d_p}{2}(\frac{\sigma_M}{\eta_M})^{1/2}$ and η_M and σ_M are respectively the viscosity and electrical conductivity of the liquid melt at a certain temperature [14].

Based on the above assumptions and Equations (1) to (5), migration velocities of the inclusions in the strong magnetic field with a high gradient are calculated by solving the following simplified Navier-Stokes equation

$$\begin{aligned}\rho_p\frac{1}{6}\pi d_p^3\frac{dv_{P,r}}{dt} &= \frac{1}{6}\pi d_p^3(\chi_M-\chi_p)\frac{1}{\mu_0}B\frac{dB}{dz}+\frac{1}{6}\pi d_p^3(\rho_p-\rho_M)g\\ &\quad -3\pi\eta_{M,B}v_{P,r}d_p\end{aligned} \tag{6}$$

2.2. Inclusion Removal from Liquid Aluminum under a Strong Magnetic Field with an Imposed DC Current

With an imposed DC current on the liquid melt, the situation is different from the one without current (see Fig. 1). In this case, an extra Lorentz force acts on the liquid melt, resulting in an electromagnetic Archimedes force (F_p^{EA} in Equation (7)) on the non-metallic inclusion due to the electrical conductivity difference between the liquid metal and the non-metallic inclusion. The force on the inclusion can be expressed by [15]

$$F_p^{EA} = -\frac{3}{2}\frac{\sigma_M-\sigma_p}{2\sigma_M+\sigma_p}J\times B \tag{7}$$

where σ_M and σ_p are the electrical conductivity of the liquid metal and the non-metallic inclusion respectively.

To simplify the calculation procedures, the following assumptions were made:

(1) The fluid flow (incompressible) is laminar and developing steady state (meanwhile, the velocities are set to zero at the walls with non-slip condition).

(2) All the physical and thermal properties of the liquid metal and the non-metallic inclusion are independent of time.
(3) The gradient of the magnetic field in the flowing direction is zero.
(4) The electromagnetic field is not influenced by the fluid flow and the induced magnetic field by the DC current is not taken into consideration in the present calculation.
(5) There is no influence of the inclusions on the fluid flow field.

As shown in Fig. 1, with the imposed DC current, an induced electromagnetic Archimedes force acts on the inclusion. The inclusion particle is pushed to one side of the channel and then trapped by the refractory wall. In this case, the migration velocity of the inclusion particle in the direction of the electromagnetic Archimedes force can be calculated by

$$\rho_p \frac{1}{6}\pi d_p^3 \frac{dv_{P,r}}{dt} = \frac{1}{6}\pi d_p^3 F_p^{EA} - 3\pi\eta_{M,B} v_{P,r} d_p \tag{8}$$

2.3. Trajectories and Removal Efficiency of Inclusion Particles

The motion of an inclusion particle can be divided into radial (r) and horizontal (z) directions (Fig. 1). To calculate the trajectories of the inclusion particles under the treatment of strong magnetic fields with and without an imposed current, the velocity in radial direction is calculated by solving the Navier-Stokes equation (Equation (6) or (8)), while the velocity in the z direction (flowing direction) can be obtained from the numerical solution of the fluid flow field by neglecting the unsteady forces. The migration velocity of the inclusion particle in the z direction is assumed to be equal to the local melt velocity. The solution of the flow field can be found in literature [16]. The particle position (r, z) in the longitudinal section of the channel as a function of time can be calculated by substituting the obtained velocities into Equation (9).

$$\begin{cases} r = r_0 + v_{P,r}dt \\ z = z_0 + v_{P,z}dt \end{cases} \tag{9}$$

where r_0 and z_0 are the initial position of the particle and $v_{P,z}$ is the particle velocity in the z direction.

Consequently, the trajectories of the inclusions in the flowing aluminium melt during the electromagnetic treatment can be predicted.

The removal efficiency is obtained by calculating the migration distance of an inclusion particle. As shown in Fig. 3, all the inclusions in the melt can be removed if the inclusion particle flowing in from

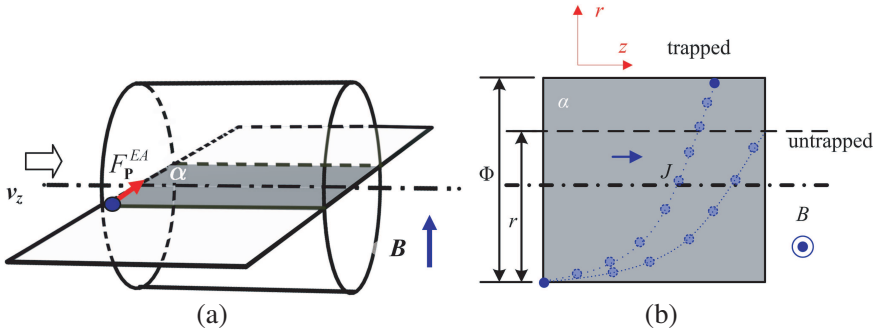

Figure 3. Principles of the inclusion removal under the treatment of magnetic field with an imposed current flow by neglecting the inclusion migration in the magnetic field direction. (a) Initial particle position in a cylindrical channel. and (b) Particle trajectory in the horizontal plane (it is similar case when there is without an DC current, only the inclusion is trapped at the bottom of the tube instead of the horizontal sidewall).

the position illustrated in the figure reaches the opposite sidewall. Therefore, the removal efficiency ξ is defined in Equation (10) to be the ratio of the particle migration distance in the radial direction, r to the diameter Φ of the cylindrical channel. The particle migrating distance in the r direction is calculated by integration of Equation (6) or Equation (8).

$$\xi = \frac{r}{\Phi} \tag{10}$$

3. RESULTS AND DISCUSSION

3.1. Inclusion Removal from Liquid Aluminium under a Strong Magnetic Field with a High Gradient

In order to investigate the effect of the magnetic field (assuming the magnetic field is independent of time t) on the migration of inclusions in aluminum melt, typical non-metallic inclusions, such as Al_2O_3, SiC, and SiO_2 were chosen [12]. The physical properties of those non-metallic inclusions at 933 K are listed in Table 1. The resultant force as well as the migration velocity of a non-metallic inclusion under the strong magnetic field with a high gradient is calculated according to Equations (1) to (6) (without imposed DC current).

The inclusion migration velocities and their time dependence for 10 µm sized Al_2O_3, SiC and SiO_2 particles at magnetic field density

of 10 T and the gradient of 60 T/m are calculated and shown in Fig. 4(a). It is clear that the velocities of all the particles reach their maximum values in a very short time (around 30 μs). Under the present calculation assumptions, the migration velocities for distinct inclusion type increase in the order: $SiO_2 < SiC < Al_2O_3$ due to the difference of their magnetic susceptibilities (Table 1).

Figure 4(b) summarises the particle type and size dependency of the ratio of maximum particle velocity in the magnetic field to that in the gravitational field (μ_m/μ_g as calculated from Equation (6) and the Stokes theory [16]). Although the ratio can reach up to more than 20 for the Al_2O_3 particles smaller than 2 μm, the influence of the magnetic field decrease rapidly with the particle size and the enhancement of inclusion removal by using a magnetic field is limited when the diameter is more than around 20 μm. This is due to the increased drag force for large inclusions under strong magnetic fields (see Equations (4) and (5)). The influence of the magnetic field is also found more pronounced in a paramagnetic melt when the diamagnetic particle is inherent with smaller magnetic susceptibility and density.

Additionally, the removal efficiency, see Equation (10), is evaluated and shown in Fig. 5. It is influenced by various factors. One of the factors is the flow rate of the liquid melt. Afshar [17] stated that the faster the melt flows, the lower the removal efficiency becomes since the decrease of the treatment duration. Here, the case with zero flow rate is considered in order to eliminate the influence of melt flowing. As illustrated in Fig. 5(a), the removal efficiency for Al_2O_3 increases

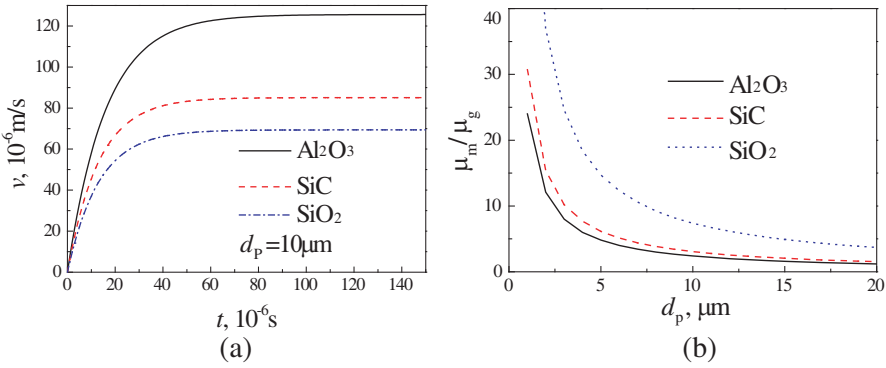

Figure 4. Migration velocities of the non-metallic inclusions in liquid aluminum under gradient magnetic field ($B = 10$ T, 60 T/m). (a) The dependence of time; (b) the ratio of the maximum velocities μ_m/μ_g with and without the magnetic field.

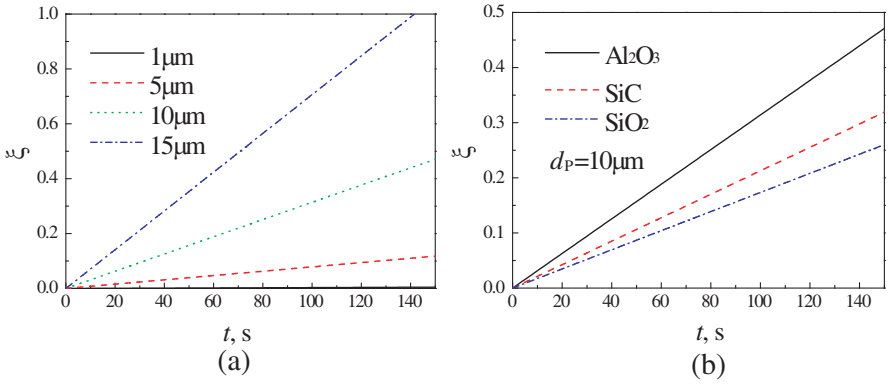

Figure 5. Effect of inclusion size and physical property on the removal efficiency under gradient magnetic field (flow rate is zero). (a) The dependence of the particle size (Al_2O_3); (b) the dependence of the physical properties.

significantly with increasing the particle size and the value is very low for inclusions with a particle size smaller than 5 μm. The influence of the inclusion type (see Table 1) is shown in Fig. 5(b). Al_2O_3 inclusion inherent with the smallest magnetic susceptibility and largest density exhibits the highest removal efficiency. However, the values are still low even after a treatment for hundred seconds compared with literature data using traditional electromagnetic methods [17, 18].

Summarizing the calculation results presented in Figs. 4 and 5, it is clear that: (1) The removal rate can not be significantly improved by using a strong magnetic field with a high gradient for large inclusions (e.g., $> 10\,\mu m$), due to a large viscosity drag force acting on the inclusion particles; (2) despite of the considerable high ratio of μ_m/μ_g (Fig. 4(b)) for small inclusions (e.g., $< 5\,\mu m$), the low removal efficiencies make it impractical to separate small inclusions from liquid aluminum by applying only a strong magnetic field with a high gradient.

3.2. Inclusion Removal from Liquid Aluminum in a Strong Magnetic Field with an Imposed Current

When imposing a DC current on the liquid aluminum, an electromagnetic Archimedes force originates and acts on the non-metallic inclusion (see Section 2.2). The force (F_p^{EA} in Equation (7)) is calculated for Al_2O_3 inclusions in an aluminum melt at 933 K as a function of the particle diameter as graphically presented in Fig. 6.

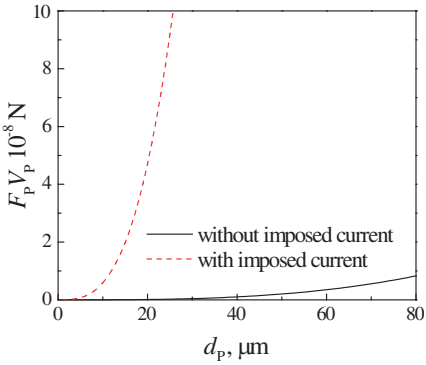

Figure 6. The driving forces of inclusion migration in the high gradient magnetic field with and without imposed DC current (1500 kA/m^2, Al_2O_3).

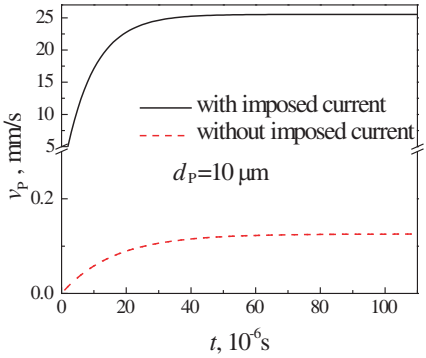

Figure 7. Time dependence of the migration velocity of Al_2O_3 inclusion under high gradient magnetic field (10 T and 60 T/m) with an imposed DC current (1500 kA/m^2).

According to the references [11, 16], the imposed DC current density for the calculations is chosen to be 1500 kA/m^2 and the magnetic field density is 10 T. Compared with the driving force in the magnetic field gradient direction (F_p in Equation (1) without the DC current), a substantially larger electromagnetic Archimedes force (Equation (7)) is acting on the inclusion in the perpendicular direction of the magnetic field gradient, see Figs. 1(c) and 3). This implies that the imposed DC current on the aluminum melt can significantly accelerate the Al_2O_3 particle migration rate in the liquid aluminum, hence improving the Al_2O_3 removal efficiency. Compared the magnitudes of F_p and F_p^{EA} in Fig. 6, the migration in the gradient direction was omitted and only the velocities of inclusions in the electromagnetic Archimedes force direction were calculated in the case with an imposed current.

Figure 7 illustrates the time dependence of the Al_2O_3 particle migration velocity in the liquid aluminum for a particle diameter of 10 μm with a DC current of 1500 kA/m^2 imposed. To simplify the calculation, only the migration in the electromagnetic Archimedes force direction was taken into account (Equation (8)). The migration velocity can reach more than 100 times that of the case without current. The removal of Al_2O_3 inclusion from an aluminum melt can therefore be tremendously improved by imposing a DC current.

To get a better understanding of the inclusion behavior in the liquid aluminum when imposing a DC current under a strong magnetic

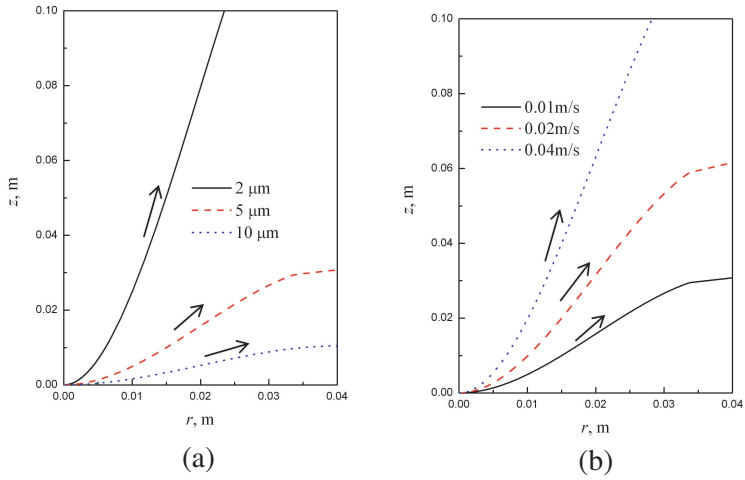

Figure 8. Effect of (a) particle size (10 T, 0.01 m/s), and (b) flowing rate (10 T, 5 μm) on the Al_2O_3 trajectories under strong magnetic field with an imposed current (1500 kA/m^2).

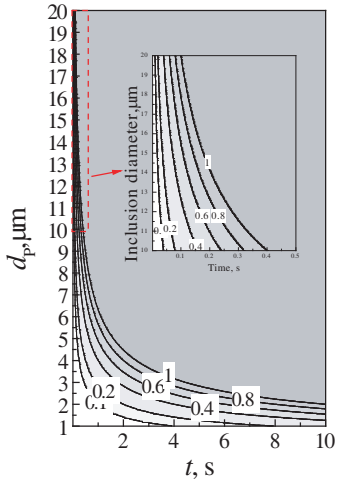

Figure 9. Contourplot of the removal efficiencies of Al_2O_3 inclusions from liquid aluminum using a strong magnetic field (10 T) with an imposed DC current (1500 kA/m^2).

field, the migrating trajectories of the Al_2O_3 inclusion in a flowing aluminum melt are calculated. Assuming that an aluminum melt containing a spherical Al_2O_3 inclusion with a specific diameter located at the position ($z = 0$, $r = 0$) in the beginning ($t = 0$) (see Fig. 3(a)), flows through the channel with a constant inlet flow rate. Then, the particle position (r, z) in the longitudinal section of the channel (Fig. 3(b)) can be calculated by solving the Equations (8) and (9).

The effects of the particle size (when the flow rate is 0.01 m/s) and the aluminum melt flow rate (the particle size is 5 μm) on the migrating trajectories of the Al_2O_3 inclusion are presented in Fig. 8. The inclusions are pushed and moved to one side of the channel where they can be trapped by the refractory wall. The results reveal that the particle size and melt flowing rate influence the trajectories significantly, indicating that larger inclusions are easier to be removed with lower flowing rate, namely, longer treatment time. Therefore, the inclusion size and the treatment time are two key factors directly affecting the removal efficiency.

The removal efficiency, calculated based on Equations (8) and (10), as a function of the particle size and treatment time is presented in Fig. 9. Compared with Fig. 5, the removal efficiency is much larger and it reaches 100% for 5 μm sized inclusions in around 2 seconds, suggesting that it is a very efficient method to remove micrometer-sized inclusions by using strong magnetic fields with an imposed DC current. In addition, the removal efficiency can be further improved by increasing the current density, which has already been investigated for the inclusion removal from magnesium melts in a rectangular channel [16]. However, the power efficiency will be much lower because of the increased Joule heat losses (proportional to J^2) and the power is consumed by heating the melt [11].

Furthermore, the DC current will induce an additional magnetic field which influences the trajectories of inclusions [16]. A further investigation is therefore required. However, the removal efficiency will be comparable since the electromagnetic Archimedes force will be hardly influenced. Based on the above calculations and discussions, an efficient method is then proposed to remove small inclusions (e.g., < 10 μm) by imposing a DC current on the liquid aluminum flow under a strong magnetic field.

4. CONCLUSION

A numerical calculation is performed to investigate the inclusion removal from a flowing aluminum melt in a cylindrical channel. The cases with and without imposed DC current are both evaluated with

respect to the inclusion removal efficiency. The following conclusions can be drawn:

1) Without applying a DC current, it is impractical to separate small inclusions from liquid aluminum by applying only the strong magnetic field with high gradient. For large inclusions (e.g, $> 10\,\mu m$), the removal rate can not be significantly improved by using the strong magnetic field with high gradient due to a large viscosity drag force acting on the inclusion particles. For small inclusions (e.g., $< 5\,\mu m$), in spite of a considerable enhancement of the migration, the removal efficiencies are still low (Fig. 5(a)).
2) With a DC current imposed (with a density of $1500\,kA/m^2$), the electromagnetic Archimedes force becomes dominant, resulting in a significant enhancement of the inclusion removal. According to the calculation, the removal efficiency reaches 100% in 2 seconds for $5\,\mu m$ inclusion.
3) The trajectories of Al_2O_3 inclusions in aluminum melt can be strongly influenced by the particle size and melt flowing rate. The results reveal that larger inclusions are easier to be removed with lower flowing rate. The inclusions are pushed and moved to one side of the channel where they can be trapped by the refractory wall.
4) An effective process can be proposed to remove small inclusions (e.g., $< 10\,\mu m$) from liquid aluminum by imposing a strong magnetic field and a DC current.

ACKNOWLEDGMENT

Financial support from of the Flemish Institute for the Promotion of Scientific Technological Research in Industry (IWT) under contract SBO-PROMAG (60056) is gratefully acknowledged.

REFERENCES

1. Makarov, S., R. Ludwig, and D. Apelian, "Electromagnetic separation techniques in metal casting. I. Conventional methods," *IEEE Magnet.*, Vol. 36, No. 4, 2015–2021, 2000.
2. Zhang, L., A. Ciftja, and L. Damoah, "Removal of non-metallic inclusions from molten aluminum," *Proceedings of EMC*, 1413–1428, 2007.
3. Fernandes, M., J. C. Pires, N. Cheung, and A. Garcia, "Investigation of the chemical composition of nonmetallic

inclusions utilizing ternary phase diagrams," *Mater. Char.*, Vol. 49, 437–443, 2003.

4. Zhou, M., D. Shu, K. Li, W. Zhang, B. Sun, J. Wang, and H. Ni, "Performance improvement of industrial pure aluminum treated by stirring molten fluxes," *Mater. Sci. Eng. A*, Vol. 347, 280–290, 2003.
5. Yoon, E., J. Kim, H. Choi, and H. Kwon, "Effects of electromagnetic force on the removal of alumina particles in molten A356 aluminum alloy," *J. Mater. Sci. Lett.*, Vol. 21, 739–742, 2002.
6. Asai, S., "Recent development and prospect of electromagnetic processing of materials," *Sci. Technol. Adv. Mater.*, Vol. 1, 191–200, 2000.
7. Sun, Z., T. Kokalj, M. Guo, F. Verhaeghe, O. Van Der Biest, B. Blanpain, and K. Van Reusel, "Effect of the strong magnetic field on the magnetic interaction between two non-magnetic particles migrating in a conductive fluid," *EPL*, Vol. 85, No. 1, 14002, 2009.
8. Takahashi, K. and S. Taniguchi, "Electromagnetic separation of nonmetallic inclusions from liquid metal by imposition of high frequency magnetic field," *ISIJ Int.*, Vol. 43, No. 6, 820–827, 2003.
9. Li, K., J. Wang, D. Shu, T. X. Li, B. D. Sun, and Y. H. Zhou, "Theoretical and experimental investigation of aluminum melt cleaning using alternating electromagnetic field," *Mater. Lett.*, Vol. 56, 215–220, 2002.
10. Gillon, P., "Uses of intense d.c. magnetic fields in materials processing," *Mater. Sci. Eng. A*, Vol. 287, 146–152, 2000.
11. Makarov, S., R. Ludwig, and D. Apelian, "Electromagnetic separation techniques in metal casting. II. Separation with superconducting coils," *IEEE Magnet.*, Vol. 37, No. 2, 1024–1031, 2000.
12. Totten, G. and M. Scott, "Physical metallurgy and processes," *Handbook of Aluminum*, Vol. 1, 665–666, Marcel Dekker, Inc., New York, 2003.
13. Sun, Z., M. Guo, T. Kokalj, O. Van Der Biest, and B. Blanpain, "Migration and interaction behavior of electrical-insulating particles in a conductive melt under strong magnetic field with high gradient," *Proceedings EPD Congress 2009*, 785–792, 2009.
14. Reitz, J. and F. Milford, *Foundations of Electromagnetic Theory*, 182–216, Addison-Wesley publishing company, Inc., London, 1962.
15. Leenov, D. and A. Kolin, "Theory of electromagnetophoresis

(I): Magnetohydrodynamic forces experienced by spherical and symmetrically oriented cylindrical particles," *J. Chem. Phys.*, Vol. 22, 683–688, 1954.

16. Gary, L., *Advanced Transport Phenomena: Fluid Mechanics and Convective Transport Processes*, Cambridge University Press, Cambridge, 2007.
17. Afshar, M., M. Aboutalebi, M. Isac, and R. Guthrie, "Mathematical modeling of electromagnetic separation of inclusions from magnesium melt in a rectangular channel," *Mater. Lett.*, Vol. 61, 2045–2049, 2007.
18. Shu, D., T. Li, B. D. Sun, Y. Zhou, J. Wang, and Z. Xu, "Numerical calculation of electromagnetic expulsive force upon nonmetallic inclusions in aluminum melt: Part I, Spherical Particles," *Metall. Mater. Trans. B*, Vol. 31, No. 6, 1527–1533, 2000.